XI International Conference on Computational Plasticity. Fundamentals and Applications
COMPLAS XI
E. Oñate, D.R.J. Owen, D. Peric and B. Suárez (Eds)

COMPUTATIONAL MODELLING OF A MULTIFIELD SINGLE-CRYSTAL GRADIENT PLASTICITY FORMULATION

C. B. HIRSCHBERGER*, B. D. REDDY†

*Institute of Continuum Mechanics
Leibniz Universität Hannover
Appelstr. 11, 30167 Hannover, Germany
e-mail: hirschberger@ikm.uni-hannover.de,

† Centre of Research in Applied Mechanics (CERECAM)
University of Cape Town, South Africa
7701 Rondebosch, South Africa
e-mail: daya.reddy@uct.ac.za, www.cerecam.uct.ac.za

Key words: Crystal plasticity, dislocations, finite deformation, size effects, finite elements.

Abstract. A model of higher-order single crystal plasticity is presented and reviewed in order to develop a corresponding finite-element framework. Contrary to the underlying model of Gurtin [Int. J. Plast. 24:702-725, 2008], here rather than the slip rate, the slip and its gradient constitute primary micro state variables. The resulting rate-dependent formulation accounts for size effects through the free energy depending on density of geometrically necessary dislocations. The relationship to multifield theories of continua with microstructure is pointed out. With the presented finite-element approach, the corresponding fully coupled initial-boundary value problem is solved monolithically, and features of the model are illustrated in two preliminary numerical examples.

1 INTRODUCTION

The size-dependent behaviour of polycrystalline materials such as metals at grain sizes of the order of tens to hundreds of microns is well documented. Such behaviour stems from heterogeneities in crystallites and arise, for example, due to the existence of grain boundaries, as well as due to impurities, inclusions, and other imperfections in the crystal lattices. The appropriate modelling of behaviour at the microstructural level requires a knowledge of the underlying dynamics of dislocations, and proper incorporation of such dynamics and associated length scales into the model. Dislocation-based crystal plasticity formulations capture size effects largely by including dislocation behaviour through an

averaged field description of dislocation populations in crystals. Some representative works in an extensive literature include [17, 9, 13, 6, 10, 12, 18]. Typically, the mutual interaction of dislocations are captured in a back-stress term that counteracts the resolved shear stress driving the flow of dislocations on the lattice glide planes.

The objective of this contribution is to develop finite element approximations of a model of single-crystal higher-order plasticity due to Gurtin [10]. The model is based on the use of geometrically necessary dislocation (GND) densities as a field variable. However, in contrast to the treatment in [10], instead of the slip rate, the slip constitutes a micro state variable. The relationship between gradient of slip and GND density is nevertheless constructed in a way that is consistent with the dissipation inequality. The slip together with macroscopic displacements are the primary unknown variables of the problem. It is shown that the formulation has a relationship to multifield theories [3, 4]. Conforming finite element approximations are based on a fully coupled, monolithic approach to solving the governing equations of the rate-dependent initial-boundary value problems. The article closes with two preliminary numerical examples.

2 A MULTIFIELD CRYSTAL PLASTICITY FRAMEWORK

The model of higher-order crystal plasticity largely follows that due to Gurtin [10].

2.1 Kinematics

The starting point for the description of kinematical relations is the standard multiplicative decomposition

$$\boldsymbol{F} = \boldsymbol{F}_{\mathrm{e}} \cdot \boldsymbol{F}_{\mathrm{p}} \tag{1}$$

of the deformation gradient $\boldsymbol{F} = \boldsymbol{\nabla}_{\boldsymbol{X}} \boldsymbol{\varphi}$ into elastic and plastic parts $\boldsymbol{F}_{\mathrm{e}}$ and $\boldsymbol{F}_{\mathrm{p}}$ respectively. Here $\boldsymbol{x} = \boldsymbol{\varphi}(\boldsymbol{X}, t)$ describes the motion from the material to the spatial configuration and $\boldsymbol{\nabla}_{\boldsymbol{X}}$ is the material gradient. The plastic deformation is assumed to be isochoric implying $\det \boldsymbol{F}_{\mathrm{p}} = 1$. It follows that $J := \det(\boldsymbol{F}) = \det \boldsymbol{F}_{\mathrm{e}} > 0$.

The spatial velocity gradient $\boldsymbol{l} = \boldsymbol{\nabla}_{\boldsymbol{x}} \boldsymbol{v}$ may be decomposed additively according to

$$\boldsymbol{l} = \dot{\boldsymbol{F}} \cdot \boldsymbol{F}^{-1} = \boldsymbol{l}_{\mathrm{e}} + \boldsymbol{F}_{\mathrm{e}} \cdot \widehat{\boldsymbol{L}}_{\mathrm{p}} \cdot \boldsymbol{F}_{\mathrm{e}}^{-1} \tag{2}$$

in which

$$\widehat{\boldsymbol{L}}_{\mathrm{p}} = \dot{\boldsymbol{F}}_{p} \boldsymbol{F}_{\mathrm{p}}^{-1} \,. \tag{3}$$

The elastic Cauchy–Green tensor

$$\widehat{\boldsymbol{C}}_{\mathrm{e}} = \boldsymbol{F}_{\mathrm{e}}^{\mathrm{t}} \cdot \boldsymbol{F}_{\mathrm{e}} = \boldsymbol{F}_{\mathrm{p}}^{-\mathrm{t}} \cdot \boldsymbol{C} \cdot \boldsymbol{F}_{\mathrm{p}}^{-1} \tag{4}$$

characterizes the deformation of the intermediate configuration, quantities in which are denoted here and henceforth by $\widehat{\square}$.

The motion of dislocations in a single crystal takes place on a set of n_S defined slip systems, whereby an orthonormal pair comprising a slip direction $\widehat{\boldsymbol{s}}^\alpha$ and slip-plane normal vector $\widehat{\boldsymbol{m}}^\alpha$ ($\alpha = 1, \dots, N$) in the intermediate configuration precisely defines the α-th system. It is useful also to introduce the Schmid (projection) tensor $\widehat{\boldsymbol{Z}}^\alpha = \widehat{\boldsymbol{s}}^\alpha \otimes \widehat{\boldsymbol{m}}^\alpha$, which is trace-free. For edge dislocations, the slip line direction $\widehat{\boldsymbol{l}}^\alpha$ is defined by $\widehat{\boldsymbol{l}}^\alpha = \widehat{\boldsymbol{m}}^\alpha \times \widehat{\boldsymbol{s}}^\alpha$, so that $\{\widehat{\boldsymbol{m}}^\alpha, \widehat{\boldsymbol{s}}^\alpha, \widehat{\boldsymbol{l}}^\alpha\}$ form a local orthonormal basis. In case of screw dislocations, the slip line and the slip direction coincide to $\widehat{\boldsymbol{s}}^\alpha$.

The plastic distortion-rate tensor $\widehat{\boldsymbol{L}}_\mathrm{p}$ is determined by the slip rates acting on each of the slip systems according to

$$\widehat{\boldsymbol{L}}_\mathrm{p} = \sum_{\alpha=1}^{n_\mathrm{S}} \dot{\gamma}^\alpha \, \widehat{\boldsymbol{s}}^\alpha \otimes \widehat{\boldsymbol{m}}^\alpha =: \sum_{\alpha=1}^{n_\mathrm{S}} \dot{\gamma}^\alpha \, \widehat{\boldsymbol{Z}}^\alpha \,. \tag{5}$$

The slip direction $\widehat{\boldsymbol{s}}^\alpha$, slip plane normal $\widehat{\boldsymbol{m}}^\alpha$ and dislocation line direction $\widehat{\boldsymbol{l}}^\alpha$ may be mapped to their counterparts $\boldsymbol{s}^\alpha$, $\boldsymbol{m}^\alpha$ and $\boldsymbol{l}^\alpha$ in the current configuration by setting

$$\boldsymbol{s}^\alpha = \boldsymbol{F}_\mathrm{e} \cdot \widehat{\boldsymbol{s}}^\alpha \,, \qquad \boldsymbol{m}^\alpha = (\boldsymbol{F}_\mathrm{e})^{-\mathrm{t}} \cdot \widehat{\boldsymbol{m}}^\alpha \,, \qquad \boldsymbol{l}^\alpha = \boldsymbol{F}_\mathrm{e} \cdot \widehat{\boldsymbol{l}}^\alpha \,. \tag{6}$$

2.1.1 Dislocation densities

The dislocations and their interactions are accounted for by fields of spatial densities of dislocations. In the spirit of Gurtin [10] we define both the total density of dislocations, $\rho^\alpha_\square$, and the – polar – density of geometrically necessary dislocations (GND), $\kappa^\alpha_\square$, per unit length, i. e.,, normalized by the Burgers vector length.

According to Nye [14], only the geometrically necessary dislocations are relevant to the occurrence of size effects. Following [2], the GND relates to the gradient of slip as

$$\dot{\kappa}^\alpha_\square = \boldsymbol{\nabla}_{\boldsymbol{x}} \dot{\gamma}^\alpha \cdot \boldsymbol{p}^\alpha = \boldsymbol{\nabla}_{\boldsymbol{X}} \dot{\gamma}^\alpha \cdot \boldsymbol{F}_\mathrm{p}^{-1} \cdot \widehat{\boldsymbol{p}}^\alpha \quad \text{with} \quad \widehat{\boldsymbol{p}}^\alpha = \begin{cases} -\widehat{\boldsymbol{s}}^\alpha & \text{for edge dislocations } (\square = \perp) \\ \widehat{\boldsymbol{l}}^\alpha & \text{for screw dislocations } (\square = \odot) \,. \end{cases} \tag{7}$$

Here a pullback from the spatial form to the intermediate configuration has been carried out. The respective subscript $\square \in \{\perp, \odot\}$ identifies either edge or screw dislocations.

Remark 1. *The formulation by Gurtin [10] bases on the slip rate ν^α as the primary micro state variable, the gradient of which corresponds to the* GND *rate. Contrarily, we assume the slip itself and its gradient as primary micro quantities, for which we develop the governing equations, the variational formulation and computational algorithm. Our choice is particularly beneficial as it reduces the complexity of the computational treatment.*

Remark 2. *In [7] the relationship between GND density and slip gradient is assumed to take the form*

$$\kappa^\alpha_\square = \widehat{\nabla} \gamma^\alpha \cdot \widehat{\boldsymbol{p}}^\alpha$$

in which $\widehat{\nabla}$ denotes the gradient with respect to the intermediate configuration. In the absence of the notion of a placement vector in the intermediate configuration, the nature of the gradient term is not clear. Likewise, a spatial relation of the form

$$\kappa_{\square}^{\alpha} = \boldsymbol{\nabla}_{\boldsymbol{x}} \gamma^{\alpha} \cdot \boldsymbol{p}^{\alpha} \,,$$

which is used by some authors, does not imply nor is implied by (7).

2.2 Free energy, dissipation inequality, stresses and microstresses

Dissipation inequality. The spatial form of the local dissipation inequality is

$$\mathcal{D} = \boldsymbol{\sigma} : \boldsymbol{l}_{\mathrm{e}} + \sum_{\alpha=1}^{n_{\mathrm{S}}} (\boldsymbol{\xi}^{\alpha} \cdot \boldsymbol{\nabla}_{\boldsymbol{x}} \dot{\gamma}^{\alpha} + \pi^{\alpha} \dot{\gamma}^{\alpha}) - J^{-1} \dot{\Psi} \geq 0 \qquad \text{in} \quad \mathcal{B}_t \,. \tag{8}$$

In the material configuration this inequality reads

$$\mathcal{D}_0 = \tfrac{1}{2} \widehat{\boldsymbol{S}}_{\mathrm{e}} : \mathcal{L}_{\boldsymbol{v}}^{\mathrm{p}}(\widehat{\boldsymbol{C}}_{\mathrm{e}}) + \sum_{\alpha=1}^{n_{\mathrm{S}}} (\boldsymbol{\xi}_0^{\alpha} \cdot \boldsymbol{\nabla}_{\boldsymbol{X}} \dot{\gamma}^{\alpha} + \pi_0^{\alpha} \dot{\gamma}^{\alpha}) - \dot{\Psi} \geq 0 \qquad \text{in} \quad \mathcal{B}_0 \tag{9}$$

with the Lie derivative $\mathcal{L}_{\boldsymbol{v}}^{\mathrm{p}}(\widehat{\boldsymbol{C}}_{\mathrm{e}}) = \boldsymbol{F}_{\mathrm{p}}{}^{-\mathrm{t}} \cdot \dot{\boldsymbol{C}} \cdot \boldsymbol{F}_{\mathrm{p}}^{-1} = \dot{\widehat{\boldsymbol{C}}}_{\mathrm{e}} + 2[\widehat{\boldsymbol{C}}_{\mathrm{e}} \cdot \widehat{\boldsymbol{L}}_{\mathrm{p}}]^{\mathrm{sym}}$ [16] and $\boldsymbol{\xi}_0^{\alpha} = \boldsymbol{F}^{-1} \cdot \boldsymbol{\xi}^{\alpha}$.

The free energy $\widehat{\Psi}$ is assumed to depend on the elastic tensor $\widehat{\boldsymbol{C}}_{\mathrm{e}}$ and the set $\vec{\kappa}$ of dislocation densities. This motivates the definition of a macrostress $\widehat{\boldsymbol{S}}_{\mathrm{e}}$ and vector microstress $\boldsymbol{\xi}_{\mathrm{en}}^{\alpha}$ according to

$$\widehat{\boldsymbol{S}}_{\mathrm{e}} = 2 \frac{\partial \widehat{\Psi}}{\partial \widehat{\boldsymbol{C}}_{\mathrm{e}}} \,, \qquad\qquad \boldsymbol{\xi}_{\mathrm{en}}^{\alpha} := J^{-1} \frac{\partial \widehat{\Psi}}{\partial \kappa_{\square}^{\alpha}} \boldsymbol{p}^{\alpha} \,. \tag{10}$$

By assuming that the microstress is purely energetic (that is, $\boldsymbol{\xi}^{\alpha} = \boldsymbol{\xi}_{\mathrm{en}}^{\alpha}$: see also [15]), the dissipation inequality (9) reduces to

$$\mathcal{D}^{\mathrm{red}} = \sum_{\alpha=1}^{n_{\mathrm{S}}} \pi^{\alpha} \dot{\gamma}^{\alpha} \geq 0 \,, \tag{11}$$

A flow rule for π^{α} will be specified later.

Macro- and micro-force balances. Balance equations are derived from a principle of virtual power [10]. The macroforce balance or equilibrium equation is expressed in terms of the first Piola-Kirchhoff stress and the referential body force $\mathbf{0}$ as

$$\mathrm{Div}\, \boldsymbol{P} + \boldsymbol{f}_0 = \mathbf{0} \quad \text{in } \mathcal{B}_0 \,. \tag{12}$$

This equation is supplemented by the boundary conditions $\boldsymbol{u} = \boldsymbol{u}^{\mathrm{p}}$ on $\partial \mathcal{B}_t^u$ and $\boldsymbol{P} \cdot \boldsymbol{N} = \boldsymbol{t}_0^{\mathrm{p}}$ on $\partial \mathcal{B}_0^p$, in which $\partial \mathcal{B}_t^u$ and $\partial \mathcal{B}_0^p$ are non-overlapping parts that cover the boundary $\partial \mathcal{B}_0$.

The microforce balance is given for each slip system α in the spatial configuration by

$$\operatorname{div} \boldsymbol{\xi}^\alpha - \pi^\alpha + \sigma^\alpha = 0 \quad \text{on } \alpha \text{ in } \mathcal{B}_t \tag{13}$$

In the material configuration this reads

$$\operatorname{Div} \boldsymbol{\xi}_0^\alpha - \pi_0^\alpha + \sigma_0^\alpha = 0 \quad \text{on } \alpha \text{ in } \mathcal{B}_0 \,. \tag{14}$$

Here σ_0^α is the resolved shear stress defined by

$$\sigma_0^\alpha = \left[\widehat{\boldsymbol{C}}_\mathrm{e} \cdot \widehat{\boldsymbol{S}}_\mathrm{e}\right] : \boldsymbol{Z}^\alpha \tag{15}$$

and $\operatorname{Div} = \boldsymbol{F}^{-1} : \boldsymbol{\nabla}_{\boldsymbol{X}}$.

Dirichlet and Neumann boundary conditions are assumed to be $\gamma^\alpha = \gamma_\mathrm{p}$ on $\partial\mathcal{B}_0^\nu$ and $\boldsymbol{\xi}_0^\alpha \cdot \boldsymbol{N} = t_0^{\xi\alpha}$ on $\partial\mathcal{B}_0^\xi$. For an overview on the choice of micro-hard and micro-free boundary conditions, see e. g., [7] and references cited in this work.

Remark 3. *The macro- and microforce balance equations may also be derived by adopting a micromorphic or microfield continuum approach [11, 3], in which the energy functional corresponding to the incremental problem is written as the sum of the free energy $\widehat{\Psi}$ and the dissipative flow potential Υ, which generates the dissipative microforce through the incremental form of the relation [15]*

$$\pi^\alpha = \frac{\partial \Upsilon}{\partial \dot{\gamma}^\alpha} \,. \tag{16}$$

2.3 Constitutive relations

Based on an underlying hyperelastic material, the crystal plasticity constitutive framework relies on the choice of a free energy and the definition of a flow rule or dissipation function.

2.3.1 Free energy

The free energy per reference volume is assumed to comprise an elastic or macro-energy $\widehat{\Psi}^\mathrm{macro}$ and a defect or micro-energy $\widehat{\Psi}^\mathrm{micro}$:

$$\widehat{\Psi} = \widehat{\Psi}^\mathrm{macro}(\widehat{\boldsymbol{C}}_\mathrm{e}) + \sum_{\alpha=1}^{n_\mathrm{S}} \widehat{\Psi}^\mathrm{micro}(\kappa_\square^\alpha) \,. \tag{17}$$

This yields the stress and energetic microstress via the definitions (10). For the sake of simplicity, latent hardening effects are neglected in the energetic part, and will instead be captured in the dissipative microforce via the flow rule .

Due to the relatively small elastic deformations in crystal plasticity, it suffices to choose for the macro-energy a St. Venant–Kirchhoff relation

$$\widehat{\Psi}^{\text{macro}} = \frac{\lambda}{8}\text{tr}^2(\widehat{\boldsymbol{C}}_{\text{e}} - \boldsymbol{I}) + \frac{1}{4}\mu[\widehat{\boldsymbol{C}}_{\text{e}} - \boldsymbol{I}]^2 \,. \tag{18}$$

However, following Gurtin [10], the micro-energy is formulated for both edge and screw dislocations as

$$\widehat{\Psi}^{\text{micro}}(\kappa^\alpha_\square) = \tfrac{1}{2}\sum_{\alpha=1}^{N_s} (C_1\kappa^\alpha_\perp)^2 + \left(C_2\kappa^\alpha_\odot\right)^2 \,. \tag{19}$$

With the choices $C_1 = \frac{\mu R^2}{8[1-\nu]}$ and $C_2 = \frac{\mu R^2}{4}$, the relation of [8] is retrieved (see [7] for the relationship between the two approaches).

2.3.2 Flow rule and slip resistance

Due to the physically well-established assumption that all dislocations are mobile all the time, hence we choose a viscoplastic flow rule. Various options are available: for example,

$$\pi^\alpha = S^\alpha \left(\frac{|\dot{\gamma^\alpha}|}{\dot{\gamma}^\alpha_0}\right)^m \text{sgn}(\pi^\alpha) \,. \tag{20}$$

The slip resistance S^α is given in [10] by the evolution equation

$$\dot{S}^\alpha = \sum_\beta h^{\alpha\beta}(\boldsymbol{S})|\dot{\gamma}^\beta| \tag{21}$$

in which $h^{\alpha\beta}$ is a matrix of hardening moduli and $\boldsymbol{S}$ denotes the array $[S_1, \ldots, S_{n_{\text{S}}}]^{\text{t}}$ for n_{S} slip systems. See also [1] for further details.

3 NUMERICAL FRAMEWORK FOR CRYSTAL PLASTICITY

A conforming finite element approximation is used to solve the initial-boundary value problem, with the displacement $\boldsymbol{u}$ and slips γ^α being the unknown variables.

Finite-element approximations. In a standard Bubnov–Galerkin approximation, the test and trial functions of both unknowns are discretized with the same shape functions: thus

$$\boldsymbol{u}^h = \sum_{J=1}^{n^u_{en}} N^u_J \boldsymbol{u}_J \,, \quad \delta\boldsymbol{u}^h = \sum_{I=1}^{n^u_{en}} N^u_I \delta\boldsymbol{u}_I \,, \quad \boldsymbol{\gamma}^h = \sum_{L=1}^{n^\gamma_{en}} N^\gamma_L \boldsymbol{\gamma}_L \,, \quad \delta\boldsymbol{\gamma}^h = \sum_{K=1}^{n^\gamma_{en}} N^\gamma_K \delta\boldsymbol{\gamma}_K \,, \tag{22}$$

with provision for different orders of interpolation of the displacement and slips.

Table 1: Algorithm for the crystal plasticity material routine

1. The approximate exponential map with a backward Euler approximations gives

$$\boldsymbol{F}_{\mathrm{p}}^{n+1} = [\boldsymbol{I} - \boldsymbol{\Lambda}^{n+1}]^{-1} \boldsymbol{F}_{\mathrm{p}}^{n} \qquad \text{where} \quad \boldsymbol{\Lambda}^{n+1} = \sum_{\alpha=1}^{n_{\mathrm{S}}} \Delta\gamma^{\alpha}\, \widehat{\boldsymbol{Z}}^{\alpha}$$

2. Obtain elastic right Cauchy–Green deformation tensor $\widehat{\boldsymbol{C}}_{\mathrm{e}}$ from

$$\boldsymbol{F}_{\mathrm{e}}^{n+1} = \boldsymbol{F}^{n+1} \cdot (\boldsymbol{F}_{\mathrm{p}}^{n+1})^{-1} \qquad \widehat{\boldsymbol{C}}_{\mathrm{e}}^{n+1} = (\boldsymbol{F}_{\mathrm{e}}^{n+1})^{\mathrm{t}} \cdot \boldsymbol{F}_{\mathrm{e}}^{n+1}$$

3. Obtain the GND density from

$$\kappa^{\alpha\, n+1} = \kappa^{\alpha n} + [\boldsymbol{\nabla}_{\boldsymbol{X}} \Delta\gamma^{\alpha} \cdot \boldsymbol{F}_{\mathrm{p}}^{-1} \cdot \widehat{\boldsymbol{s}}^{\alpha}]^{n+1}$$

4. Obtain the stress, microstress and resolved shear stress from

$$\widehat{\boldsymbol{S}}_{\mathrm{e}}^{n+1} = 2\frac{\partial \Psi}{\partial \widehat{\boldsymbol{C}}_{\mathrm{e}}^{n+1}}, \quad \boldsymbol{\xi}_0^{\alpha\, n+1} = (J^{n+1})^{-1} (\boldsymbol{F}^{n+1})^{-1} \left(\frac{\partial \Psi}{\partial \kappa^{\alpha}}\right)^{n+1}, \quad \sigma_0^{\alpha\, n+1} = \left[\widehat{\boldsymbol{C}}_{\mathrm{e}}^{n+1} \cdot \widehat{\boldsymbol{S}}_{\mathrm{e}}^{n+1}\right] : \widehat{\boldsymbol{Z}}^{\alpha}$$

3. Obtain the microforce π_0^{α} from the evolution

$$\pi^{\alpha\, n+1} = S^{\alpha} \left(\frac{|\Delta\gamma^{\alpha}|}{\Delta t\, \dot{\gamma}_0^{\alpha}}\right)^{m} \operatorname{sgn} \pi^{\alpha}$$

Finite-element residual and iterative solution. A spatial discretization of the weak form of the macro and micro balance (12) and (14) yields the element residuals

$$\mathbf{r}_{0I}^{u\,h}(\boldsymbol{u}^h) = \mathbf{f}_{0\mathrm{int}I}^{u\,h} - \mathbf{f}_{0\mathrm{sur}I}^{u\,h} - \mathbf{f}_{0\mathrm{vol}I}^{u\,h} \doteq \mathbf{0} \tag{23}$$

$$\mathbf{r}_{0K}^{\gamma\alpha\,h}(\gamma^{\alpha h}) = \mathbf{f}_{0\mathrm{int}K}^{\gamma\alpha\,h} - \mathbf{f}_{0\mathrm{sur}K}^{\gamma\alpha\,h} \doteq \mathbf{0} \tag{24}$$

that have to vanish at equilibrium. The internal and external macro forces at nodes I are assembled from the element contributions, which from the weak form of (12) are

$$\mathbf{f}_{\mathrm{int}I}^{u\,h} = \operatorname*{\mathbf{A}}_{e=1}^{n_{\mathrm{el}}} \int_{\mathcal{B}_0} \boldsymbol{P} \cdot \boldsymbol{\nabla}_{\boldsymbol{X}} N_I^u \,\mathrm{d}V, \quad \mathbf{f}_{\mathrm{sur}I}^{u\,h} = \operatorname*{\mathbf{A}}_{e=1}^{n_{\mathrm{el}}} \int_{\partial\mathcal{B}_0} \boldsymbol{t}_0\, N_I^u \,\mathrm{d}A, \quad \mathbf{f}_{\mathrm{vol}I}^{u\,h} = \operatorname*{\mathbf{A}}_{e=1}^{n_{\mathrm{el}}} \int_{\mathcal{B}_0} \boldsymbol{f}_0\, N_I^u \,\mathrm{d}V \tag{25}$$

Likewise, the internal and external micro forces stemming from (14) for each slip system α are determined at nodes K as

$$\mathbf{f}_{\mathrm{int}K}^{\gamma\alpha\,h} = \operatorname*{\mathbf{A}}_{e=1}^{n_{\mathrm{el}}} \int_{\mathcal{B}_0} \boldsymbol{\xi}_0^{\alpha} \cdot \boldsymbol{\nabla}_{\boldsymbol{X}} N_K^{\gamma} + [\pi_0^{\alpha} - \sigma_0^{\alpha}]\, N_K^{\gamma} \,\mathrm{d}V \qquad \alpha = 1, \ldots, n_S \tag{26}$$

$$\mathbf{f}_{\mathrm{sur}K}^{\gamma\alpha\,h} = \operatorname*{\mathbf{A}}_{e=1}^{n_{\mathrm{el}}} \int_{\partial\mathcal{B}_0} \boldsymbol{t}_0^{\xi}\, N_K^{\gamma} \,\mathrm{d}A \qquad \alpha = 1, \ldots, n_S \tag{27}$$

The energetic stresses $\boldsymbol{P}$ and $\boldsymbol{\xi}_0^{\alpha}$ are obtained from the free energy (10). The Schmid stress (15) and the dissipative micro force (20) follow from an Euler-backward time integration for the update on the plastic deformation, as summarized in Table 1.

With these ingredients, the time-dependent problem is solved incrementally for the unknown $\boldsymbol{u}$ and γ^α using an iterative global Newton-Raphson iterative solution procedure

$$\begin{bmatrix} \mathrm{D}_{\boldsymbol{u}_J}\mathbf{r}_{0I}^{u\,h} & \mathrm{D}_{\boldsymbol{\gamma}_L}\mathbf{r}_{0I}^{u\,h} \\ \mathrm{D}_{\boldsymbol{u}_J}\mathbf{r}_{0K}^{\gamma\alpha\,h} & \mathrm{D}_{\boldsymbol{\gamma}_L}\mathbf{r}_{0K}^{\gamma\alpha\,h} \end{bmatrix} \cdot \begin{bmatrix} \Delta\boldsymbol{u}_J \\ \Delta\boldsymbol{\gamma}_L \end{bmatrix} = - \begin{bmatrix} \mathbf{r}_I^u \\ \mathbf{r}_K^\gamma \end{bmatrix} \tag{28}$$

with tangent stiffness matrices $\mathrm{D}_\bullet\mathbf{r}_0^\circ$ quantifying the sensitivity of the nodal residua $\circ \in \{u, \gamma^\alpha\}$ with respect to the nodal unknowns $\bullet \in \{\boldsymbol{u}, \gamma^\alpha\}$.

4 NUMERICAL EXAMPLES

The numerical algorithm for the present crystal plasticity framework is demontrated in two benchmark-type problems. At this stage, the simulations are restricted to single slip, with a extension to multiple slip as part of future work.

4.1 Single slip in a shear layer

We first study a shear layer with one slip system under an angle of $\theta = \pi/3$, similar to the problem studied for example in [12]. Omitting periodic boundary conditions, a slip profile with little boundary influences is produced by choosing a relative broad shear layer. Unit values are used for material parameters in these preliminary computations.

Macroscopically, a lateral displacement u_1 is prescribed at top and bottom in opposite directions, and homogeneous Neumann boundary conditions are prescribed on the other two sides. To mimic the dislocation distribution within the shear layer, homogeneous micro Dirichlet, i. e.,*"micro-hard"* boundary conditions, $\gamma = 0$, are chosen at the top and bottom boundary. On the other hand the left and right boundaries obey homogenous micro Neumann boundary conditions, $t^{\xi\alpha} = 0$, often referred to as *"micro free"*.

Neglecting the lateral boundary region, we concentrate on the central region of the boundary value problem. Within the shear layer with approximately homogeneous macro deformation, the shear problem correctly reflects the zero slip at the boundaries and a non zero slip over the height profile of the shear layer. Moreover, the GND density is larger near the boundaries which reflects the pile-up of positive and negative dislocations against a dislocation-impenetrable boundary.

4.2 Single slip in a micro composite

The typical example of a model composite presented in [5] comprises a composite material with rectangular elastic particles embedded in a plastically deforming matrix. Such a double-symmetric problem can be reduced to the symmetric unit cell shown in 2(a). The elastic inclusions are modelled by prescribing zero slip within these subdomains, and the cell is subjected to simple shear loading.

While the macroscopic displacement exhibits a slightly heterogeneous deformation, the slip is, naturally, zero within the elastic inclusions and strongly heterogenous in the plastic matrix material. The slip particularly localizes horizontally just above and below

the inclusion. Due to the limitation to single slip and the modelling of gliding mechanisms only, dislocations from the left bottom cannot propagate to the top right region (Fig. 2(e)). Instead dislocations pile up against the elastic inclusions with different signs, as shown in 2(f).

5 CONCLUSION

In this short contribution, we present a multifield-type single crystal plasticity theory at finite strain, similar to the formulation of [10]. The presented governing equations stem from the choice of the the displacement, the plastic slip (rather than its rate [10]) and its gradient as the primary macro and micro state variables. With a thermodynamically consistent relationship between dislocation density rate and slip rate, the free energy, however, is formulated in terms of the GND density, which is directly related to the gradient of slip. For this framework we provide a corresponding finite-element framework that employs both the displacement and the plastic slip as primary nodal degrees of freedom and hence is a strongly coupled problem. Results based on initial computations indicate that the fully coupled algorithm based on a conforming finite element framework is robust. Current work is concerned with the extension to multiple slip, and the use of alternative forms of the hardening law based on total dislocation densities.

References

[1] R. J. Asaro and A. Needleman. Texture development and strain hardening in rate dependent polycrystals. *Acta Metall.*, 33:923–953, 1985.

[2] M. F. Ashby. The deformation of plastically non-homogeneous materials. *Phil. Mag.*, 21:399–424, 1970.

[3] G. Capriz. Continua with latent microstructure. *Arch. Rat. Mech. Anal.*, 90:43–56, 1985.

[4] G. Capriz. *Continua with Microstructure*. Springer, 1989.

[5] H. H. M. Cleveringa, E. van der Giessen, and A. Needleman. Comparison of discrete dislocation and continuum plasticity predictions for a composite material. *Acta Mater.*, 45:3163–3179, 1997.

[6] M. Ekh, M. Grymer, K. Runesson, and T. Svedberg. Gradient crystal plasticity as part of the computational modelling of polycrystals. *Int. J. Numer. Meth. Engng*, 72:197–220, 2007.

[7] I. Ertürk, J. A. W. Dommelen, and M. G. D. Geers. Energetic dislocation interactions and thermodynamical aspects of strain gradient crystal plasticity theories. *J. Mech. Phys. Solids*, 57:1801–1814, 2009.

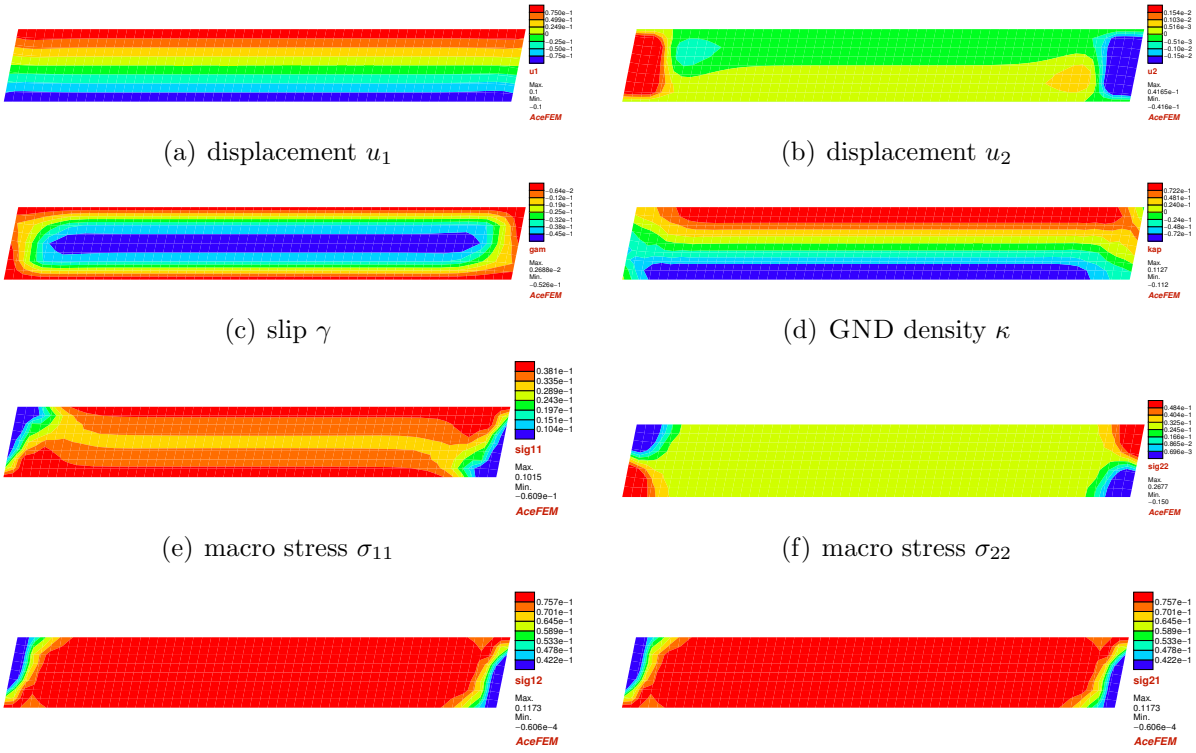

(a) displacement u_1 (b) displacement u_2

(c) slip γ (d) GND density κ

(e) macro stress σ_{11} (f) macro stress σ_{22}

(g) macro stress σ_{12} (h) macro stress σ_{21}

Figure 1: Shear layer with single slip at $\theta = 60$ and micro-hard boundary conditions for the slip.

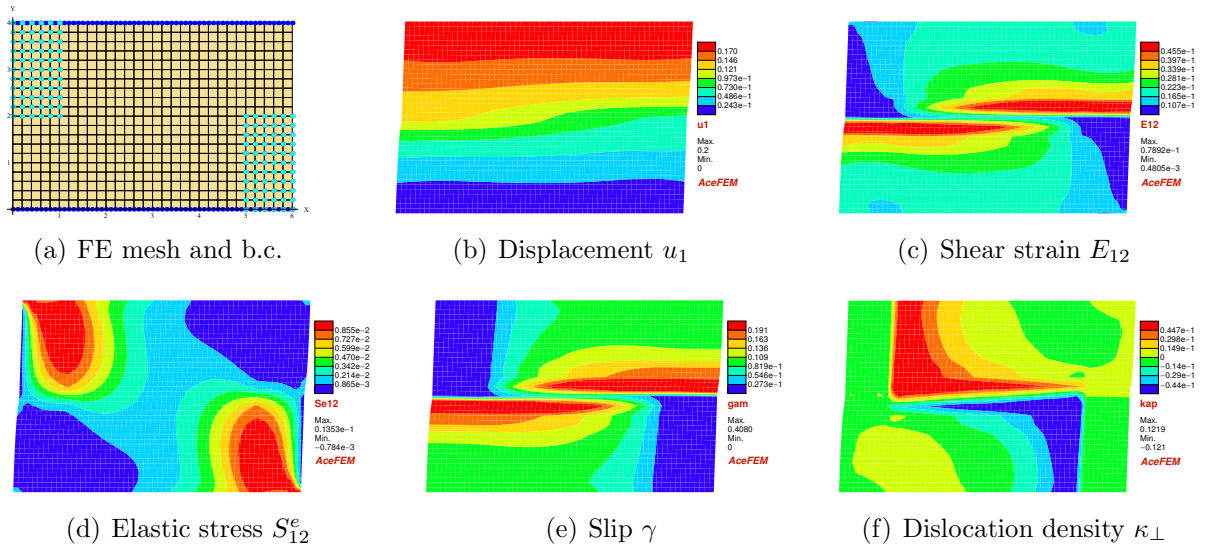

(a) FE mesh and b.c. (b) Displacement u_1 (c) Shear strain E_{12}

(d) Elastic stress S^e_{12} (e) Slip γ (f) Dislocation density $\kappa_\perp$

Figure 2: Micro composite unit cell with elastic inclusions and single slip at $\theta = 0$.

[8] L. P. Evers, W. A. M. Brekelmans, and M. G. D. Geers. Scale dependent crystal plasticity framework with dislocation density and grain boundary effects. *Int. J. Solid Struct.*, 41:5209–5230, 2004.

[9] L. P. Evers, W. A. M. Brekelmans, and M. G. D. Geers. Non-local crystal plasticity model with intrinsic SSD and GND effects. *J. Mech. Phys. Solids*, 52:2379–2401, 2004.

[10] M. E. Gurtin. A finite-deformation, gradient theory of single-crystal plasticity with free energy dependent on densities of geometrically necessary dislocations. *Int. J. Plast.*, 24:702–725, 2008.

[11] C. B. Hirschberger and P. Steinmann. Classification of concepts in thermodynamically consistent generalised plasticity. *J. Eng. Mechanics*, 135:156–170, 2009.

[12] M. Kuroda and V. Tvergaard. On the formulations of higher-order strain gradient crystal plasticity models. *J. Mech. Phys. Solids*, 56:1591–1608, 2008.

[13] A. Ma, F. Roters, and D. Raabe. A dislocation density based constitutive model for crystal plasticity fem including geometrically necessary dislocations. *Acta Mater.*, 54:2169–2179, 2006.

[14] J. F. Nye. Some geometrical relations in dislocated crystals. *Acta Metall.*, 1:153–162, 1953.

[15] B. D. Reddy. The role of dissipation and defect energy in variational formulations. Part 2: Single-crystal plasticity. *In review.*

[16] P. Steinmann and E. Stein. On the numerical treatment and analysis of finite deformation ductile single crystal plasticity. *Comput. Methods Appl. Mech. Engrg.*, 129: 235–254, 1996.

[17] B. Svendsen. On the modelling of anisotropic elastic and inelastic material behaviour at large deformation. *Int. J. Solid Struct.*, 38:9579–9599, 2001.

[18] T. Yalcinkaya, W. A. M. Brekelmans, and M. G. D. Geers. Deformation patterning driven by rate dependent non-convex strain gradient plasticity. *J. Mech. Phys. Solids*, 59:1–17, 2011.